RADIATIVE TRANSFER EQUATION IN SPHERICALLY-SYMMETRIC NON-SCATTERING MEDIA

A. PERAIAH and B. A. VARGHESE

Indian Institute of Astrophysics, Bangalore, India

(Received 4 June, 1984)

Abstract. We solved the equation of radiative transfer in spherically-symmetric shells with arbitrary internal sources. We integrated the equation of transfer on the discrete grid of angle and radius given by $[\mu_{j-1}, \mu_j]$ $[r_{i-1}, r_i]$. The size in the angle coordinates is determined by the roots of a quadrature formula where as the size in the radial coordinate is determined by the non-negativity of the reflection and transmission operators. We considered two cases of variation of the Planck function. (1) Constant throughout the medium and (2) varying as $1/r^2$. We find that in the inner shells, the radiation directed toward the centre of the sphere is more than that directed away from the centre of the sphere. In the outer shells the converse is true.

1. Introduction

There are different methods of solving the equation of radiative transfer. Each of these methods depends upon the physics of the problem for which it is designed. We encounter many situations where speed is necessary while accuracy is not so essential and in few cases we need both speed and accuracy in calculating the radiation field in a given physical situation. We have developed a technique in the framework of discrete space theory which is as accurate as any machine can provide (see Peraiah, 1984). However, the accuracy of this method depends upon the size of the radial grid. The size of the basic cell is chosen so that we always obtain non-negative reflection and transmission operators and this size is too small for an optically thick medium. Therefore, calculations of the radiation field in such media becomes time consuming although one obtains highly accurate results. However, there are situations in which both speed and accuracy are required. We must find a method which can give a larger mesh size so that computations can be speeded up sufficiently without loosing on the accuracy. We present such a method in Section 2.

2. Method of the Solution

The equation of radiative transfer in spherical symmetry is written as

$$\mu \frac{\partial I(r, \mu)}{\partial r} + \frac{1 - \mu^2}{r} \frac{\partial I(r, \mu)}{\partial \mu} = K(r) [s(r, \mu) - I(r, \mu)] ; \tag{1}$$

and for oppositely directed beam of rays,

$$-\mu \frac{\partial I(r, -\mu)}{\partial r} - \frac{1 - \mu^2}{r} \frac{\partial I(r, -\mu)}{\partial \mu} = K(r) [(s(r, -\mu) - I(r, -\mu)] , \tag{2}$$

Astrophysics and Space Science **107** (1984) 177–190. 0004–640X/84/1071–0177$02.10.

where $I(r, \mu)$ is the specific intensity of the ray making an angle $\cos^{-1}\mu$ with the radius-vector at the radial point r. The quantity $K(r)$ is the absorption parameter and $s(r, \pm\mu)$ is the source function given by

$$s(r, \mu) = \{1 - \varpi(r)\}\, b(r, \mu) + \tfrac{1}{2}\varpi(r) \int_{-1}^{+1} P(r, \mu, \mu')I(r, \mu')\, \mathrm{d}\mu' , \tag{3}$$

where $\varpi(r)$ is the albedo for single scattering, $b(r, \mu)$ is the Planck function. This quantity is assumed in advance as a function of the radial coordinate. The quantity $P(r, \mu, \mu')$ is the isotropic phase function. In this paper, we neglect scattering by setting $\varpi(r) = 0$.

We shall write

$$U(r, \mu) = 4\pi r^2 I(r, \mu) , \quad S(r, \mu) = 4\pi r^2 S(r, \mu) \quad \text{and} \quad B(r, \mu) = 4\pi r^2 b(r, \mu) . \tag{4}$$

Substituting Equations (4) into Equations (1) and (2), we obtain

$$\mu \frac{\partial U(r, \mu)}{\partial r} + \frac{1}{r}\frac{\partial}{\partial \mu}\{(1 - \mu^2)U(r, \mu)\} = K(r)\{S(r, \mu) - U(r, \mu)\} \tag{5}$$

and

$$-\mu \frac{\partial U(r, -\mu)}{\partial r} - \frac{1}{r}\frac{\partial}{\partial \mu}\{(1 - \mu^2)U(r, -\mu)\} = K(r)\{S(r, -\mu) - U(r, -\mu)\} . \tag{6}$$

Equations (5) and (6) are integrated over the radius-angle mesh bounded by $[r_i, r_{i-1}]$ $[\mu_j, \mu_{j-1}]$ (see Figure 1) where μ's are the roots of a quadrature formula. We solve Equations (5) and (6) following Lathrop and Carlson (1967, 1971).

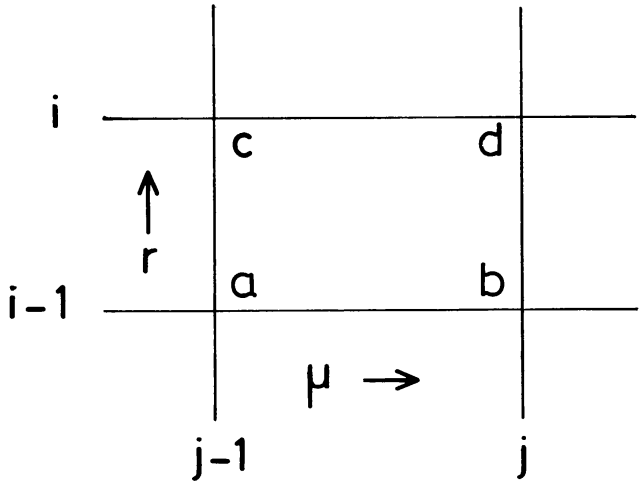

Fig. 1. Schematic diagram of the radius-angle mesh.

The specific intensity is expressed by the interpolation formula of the form

$$U(r,\mu) = U_{00} + U_{01}\xi + U_{10}\eta + U_{11}\xi\eta\,, \tag{7}$$

where

$$\xi = \frac{r - \bar{r}}{\Delta r/2}\,, \tag{8}$$

$$\eta = \frac{\mu - \bar{\mu}}{\Delta\mu/2}\,, \tag{9}$$

$$\bar{r} = \tfrac{1}{2}(r_i + r_{i-1})\,, \qquad \Delta r = (r_i - r_{i-1})\,, \tag{10}$$

$$\bar{\mu} = \tfrac{1}{2}(\mu_j + \mu_{j-1})\,, \qquad \Delta\mu = (\mu_j - \mu_{j-1})\,. \tag{11}$$

The interpolation coefficients U_{00}, U_{01}, U_{10}, and U_{11} can be expressed in term of the nodal values of $U(r,\mu)$, i.e., U_a, U_b, U_c, and U_d. Substituting Equation (7) in Equations (5) and (6) we obtain

$$\frac{2\mu}{\Delta r}\,[U_{01} + U_{11}\eta] + \frac{1-\mu^2}{r}\,\frac{2}{\Delta\mu}\,[U_{10} + U_{11}\xi] - \frac{2\mu}{r}\times$$
$$\times\,[U_{00} + U_{01}\xi + U_{10}\eta + U_{11}\xi\eta] = K(r)\times$$
$$\times\,[S(r,\mu) - U_{00} - U_{01}\xi - U_{10}\eta - U_{11}\xi\eta]\,. \tag{12}$$

Next, we apply the operators

$$\alpha = \frac{1}{\Delta\mu}\int_{\Delta\mu} \ldots \mathrm{d}\mu \tag{13}$$

and

$$\beta = \frac{1}{V}\int_{\Delta r} \ldots 4\pi r^2\,\mathrm{d}r\,, \tag{14}$$

successively on Equation (12) and obtain

$$\frac{2}{\Delta r}\left[\bar{\mu}U_{01} + \frac{1}{6}\,\Delta\mu U_{11}\right] + \frac{2}{\Delta\mu}\,\frac{1-\overline{\mu^2}}{\Delta r}\,\frac{1}{2}\,\frac{\Delta A}{\bar{A}}\left[U_{10} + \frac{1}{6}\,\frac{\Delta r}{\bar{r}}\,U_{11}\right] -$$
$$-\,\bar{\mu}U_{00}\,\frac{\Delta A}{V} + \frac{2\bar{\mu}U_{01}}{\Delta r}\left[\bar{r}\,\frac{\Delta A}{V} - 2\right] -$$
$$-\,\frac{1}{6}\,\Delta\mu U_{10}\,\frac{\Delta A}{V} + \frac{1}{3}\,\frac{\Delta\mu}{\Delta r}\,U_{11}\left(\bar{r}\,\frac{\Delta A}{V} - 2\right) =$$

$$= K(r)\left[S_{00} + \frac{1}{6}\frac{\Delta A}{\bar{A}}\,S_{01} - U_{00} - \frac{1}{6}\frac{\Delta A}{\bar{A}}\,U_{01}\right], \tag{15}$$

where we have approximated the source function in the some manner as we did to the specific intensity $U(r, \mu)$ given in Equation (7). Furthermore,

$$V = \tfrac{4}{3}\pi(r_i^3 - r_{i-1}^3)\,, \tag{16}$$

$$\overline{\mu^2} = (\bar{\mu})^2 + \frac{(\Delta\mu)^2}{12}\,, \tag{17}$$

$$\bar{A} = \frac{V}{\Delta r}\,, \tag{18}$$

$$\Delta A = 4\pi(r_i^2 - r_{i-1}^2)\,. \tag{19}$$

The interpolation coefficients U_{00}, U_{01}, etc., can be expressed by the nodal values as

$$U_{00} = \tfrac{1}{4}(+U_a + U_b + U_c + U_d)\,, \qquad U_{01} = \tfrac{1}{4}(-U_a - U_b + U_c + U_d)\,,$$
$$U_{10} = \tfrac{1}{4}(-U_a + U_b - U_c + U_d)\,, \qquad U_{11} = \tfrac{1}{4}(+U_a + U_b - U_c + U_d)\,. \tag{20}$$

Substituting Equations (20) in Equation (15) and a similar equation corresponding to Equation (6), we obtain

$$-\left[\mu_{j-1/2}^{-}(1+q) - \tfrac{1}{2}\tau\left(1 - \frac{1}{6}\frac{\Delta A}{\bar{A}}\right) + \frac{1}{2}\frac{1-\overline{\mu^2}}{\Delta\mu}\frac{\Delta A}{\bar{A}}\left(1 - \frac{1}{6}\frac{\Delta r}{\bar{r}}\right)\right]U_a -$$

$$-\left[\mu_{j-1/2}^{+}(1+q) - \tfrac{1}{2}\tau\left(1 - \frac{1}{6}\frac{\Delta A}{\bar{A}}\right) - \frac{1}{2}\frac{1-\overline{\mu^2}}{\Delta\mu}\frac{\Delta A}{\bar{A}}\left(1 - \frac{1}{6}\frac{\Delta r}{\bar{r}}\right)\right]U_b +$$

$$+\left[\mu_{j-1/2}^{-}(1+p) + \tfrac{1}{2}\tau\left(1 + \frac{1}{6}\frac{\Delta A}{\bar{A}}\right) - \frac{1}{2}\frac{1-\overline{\mu^2}}{\Delta\mu}\frac{\Delta A}{\bar{A}}\left(1 + \frac{1}{6}\frac{\Delta r}{\bar{r}}\right)\right]U_c +$$

$$+\left[\mu_{j-1/2}^{+}(1+p) + \tfrac{1}{2}\tau\left(1 + \frac{1}{6}\frac{\Delta A}{\bar{A}}\right) + \frac{1}{2}\frac{1-\overline{\mu^2}}{\Delta\mu}\frac{\Delta A}{\bar{A}}\left(1 + \frac{1}{6}\frac{\Delta r}{\bar{r}}\right)\right]U_d =$$

$$= \tfrac{1}{2}\tau\left[\left(1 - \frac{1}{6}\frac{\Delta A}{\bar{A}}\right)(S_a + S_b) + \left(1 + \frac{1}{6}\frac{\Delta A}{\bar{A}}\right)(S_c + S_d)\right] \tag{21}$$

and

$$+\left[\mu_{j-1/2}^{-}(1-q) + \tfrac{1}{2}\tau\left(1 - \frac{1}{6}\frac{\Delta A}{\bar{A}}\right) + \frac{1}{2}\frac{1-\overline{\mu^2}}{\Delta\mu}\frac{\Delta A}{\bar{A}}\left(1 - \frac{1}{6}\frac{\Delta r}{\bar{r}}\right)\right]U_a +$$

$$+\left[\mu_{j-1/2}^{-}(1-q) + \tfrac{1}{2}\tau\left(1 - \frac{1}{6}\frac{\Delta A}{\bar{A}}\right) - \frac{1}{2}\frac{1-\overline{\mu^2}}{\Delta\mu}\frac{\Delta A}{\bar{A}}\left(1 - \frac{1}{6}\frac{\Delta r}{\bar{r}}\right)\right]U_b -$$

$$-\left[\mu^{-}_{j-1/2}(1-p)-\tfrac{1}{2}\tau\left(1+\frac{1}{6}\frac{\Delta A}{\bar{A}}\right)-\frac{1}{2}\frac{1-\overline{\mu^2}}{\Delta\mu}\frac{\Delta A}{\bar{A}}\left(1+\frac{1}{6}\frac{\Delta r}{\bar{r}}\right)\right]U_c -$$

$$-\left[\mu^{+}_{j-1/2}(1-p)-\tfrac{1}{2}\tau\left(1+\frac{1}{6}\frac{\Delta A}{\bar{A}}\right)+\frac{1}{2}\frac{1-\overline{\mu^2}}{\Delta\mu}\frac{\Delta A}{\bar{A}}\left(1+\frac{1}{6}\frac{\Delta r}{\bar{r}}\right)\right]U_d =$$

$$=\tfrac{1}{2}\tau\left[\left(1-\frac{1}{6}\frac{\Delta A}{\bar{A}}\right)(S_a+S_b)+\left(1+\frac{1}{6}\frac{\Delta A}{\bar{A}}\right)(S_c+S_d)\right], \tag{22}$$

where

$$\tau = K\Delta r\,, \tag{23}$$

$$\mu^{+}_{j-1/2} = \bar{\mu}\left(1+\frac{1}{6}\frac{\Delta\mu}{\bar{\mu}}\right) = \tfrac{1}{3}(2\mu_j+\mu_{j-1})\,, \tag{24}$$

$$\mu^{-}_{j-1/2} = \bar{\mu}\left(1-\frac{1}{6}\frac{\Delta\mu}{\bar{\mu}}\right) = \tfrac{1}{3}(\mu_j+2\mu_{j-1})\,, \tag{25}$$

$$p = \frac{\bar{r}}{\Delta r}\frac{\Delta A}{\bar{A}}-\frac{1}{2}\frac{\Delta A}{\bar{A}}-2\,, \tag{26}$$

$$q = 2-\frac{1}{2}\frac{\Delta A}{\bar{A}}-\frac{\bar{r}}{\Delta r}\frac{\Delta A}{\bar{A}}\,. \tag{27}$$

We shall define the following quantities:

$$t = \Delta r/\bar{r} = (r_i-r_{i-1})/\tfrac{1}{2}(r_i+r_{i-1})\,; \tag{28}$$

and, for $t \ll 1$, we have

$$\frac{\Delta A}{\bar{A}} = \frac{2t}{(1+\frac{1}{12}t^2)} \approx 2t\,, \tag{29}$$

$$1\pm\frac{1}{6}\frac{\Delta A}{\bar{A}} = (1+\tfrac{1}{3}t+\tfrac{1}{12}t^2)/(1\pm\tfrac{1}{12}t^2) \approx 1\pm\tfrac{1}{3}t\,, \tag{30}$$

$$p \approx q \approx -t\,,$$

$$\tau^{\pm}_{i-1/2} = \tau_{i-1/2}\left(1\pm\frac{1}{6}\frac{\Delta A}{\bar{A}}\right), \tag{31}$$

$$\rho^{i-1/2,\,\pm}_{j-1/2} = \frac{1}{2}\frac{1-\overline{\mu^2}}{\Delta\mu}\frac{\Delta A}{\bar{A}}\left(1\pm\frac{1}{6}\frac{\Delta r}{\bar{r}}\right). \tag{32}$$

The source terms are written as

$$S^{i,+} = (1 - \varpi_i)B^{i,+} + \tfrac{1}{2}\varpi_i[P_i^{+\,+} CU^{i,+} + P_i^{+\,-} CU^{i,-}]\,; \tag{33}$$

similarly $S^{i-1,+}$; where C's are the angle quadrature weights. The phase function $P^{+\,+}$, $P^{+\,-}$ are given by

$$P_i^{+\,+} = P(r_i, +\mu_j, +_j)\,, \tag{34}$$

$$P_i^{+\,-} = P(r_i, +\mu_j, -\mu_j)\,; \tag{35}$$

and

$$U^{i,\pm} = U(r_i, \pm\mu_j)\,, \tag{36}$$

$$\mathbf{M}^{+}{}_{p} = (1 + p)\mathbf{M}\,, \qquad \mathbf{M}^{-}{}_{p} = (1 - p)\mathbf{M}\,, \tag{37}$$

$$\mathbf{M}_q^{+} = (1 + q)\mathbf{M}\,, \qquad \mathbf{M}_q^{-} = (1 - q)\mathbf{M}\,, \tag{38}$$

$$\mathbf{M} = \begin{bmatrix} \mu_{1/2}^{-} & \mu_{1/2}^{+} & & & & \\ & \mu_{3/2}^{-} & \mu_{3/2}^{+} & & & \\ & & \ddots & \ddots & & \\ & & & \mu_{j-1/2}^{-} & \mu_{j-1/2}^{+} & \\ & & & & \mu_J & \end{bmatrix} \tag{39}$$

and

$$\boldsymbol{\rho}^{\pm} = \begin{bmatrix} \rho_{1/2}^{\pm} & -\rho_{1/2}^{\pm} & & & & \\ & \rho_{3/2}^{\pm} & -\rho_{3/2}^{\pm} & & & \\ & & \ddots & \ddots & & \\ & & & \rho_{j-1/2}^{\pm} & -\rho_{j-1/2}^{\pm} & \\ & & & & 0 & \end{bmatrix}, \tag{40}$$

$$\mathbf{Q} = \begin{bmatrix} 1 & 1 & & & & \\ & 1 & 1 & & & \\ & & 1 & 1 & & \\ & & & \ddots & \ddots & \\ & & & & 1 & 1 \\ & & & & & 1 \end{bmatrix}, \tag{41}$$

$$\boldsymbol{\gamma}^{+\,+} = \tfrac{1}{2}\varpi\mathbf{p}^{+\,+}\,C\,,$$

$$\boldsymbol{\gamma}^{+\,-} = \tfrac{1}{2}\varpi\mathbf{p}^{+\,-}\,C, \quad \text{etc.}\,, \tag{42}$$

$$\bar{\boldsymbol{\rho}}_{\pm} = \mathbf{Q}^{-1}\,\boldsymbol{\rho}^{\pm}\,,$$

$$\mathbf{M}_1 = \mathbf{Q}^{-1} M_p^+ ,$$
$$\mathbf{M}_2 = \mathbf{Q}^{-1} M_p^- ,$$
$$\mathbf{M}_3 = \mathbf{Q}^{-1} M_q^+ , \tag{43}$$
$$\mathbf{M}_4 = \mathbf{Q}^{-1} M_q^- .$$

Now, we can rewrite Equations (21) and (22) using the quantities defined in Equations (28) to (43). We thus obtain for the J angles the relations

$$[\mathbf{M}_1 - \bar{\boldsymbol{\rho}}_+ + \tfrac{1}{2}\tau^+(\mathbf{I} - \boldsymbol{\gamma}^{++})]\mathbf{U}_i^+ - [\mathbf{M}_3 + \bar{\boldsymbol{\rho}}_- - \tfrac{1}{2}\tau^-(\mathbf{I} - \boldsymbol{\gamma}^{++})]\mathbf{U}_{i-1}^+ =$$
$$= \tau(1 - \varpi)\mathbf{B}^+ + \tfrac{1}{2}\tau^- \boldsymbol{\gamma}^{+-}\mathbf{U}_{i-1}^- + \tfrac{1}{2}\tau^+ \boldsymbol{\gamma}^{+-}\mathbf{U}_i^- \tag{44}$$

and

$$-[\mathbf{M}_2 - \bar{\boldsymbol{\rho}}_+ - \tfrac{1}{2}\tau^+(\mathbf{I} - \boldsymbol{\gamma}^{--})]\mathbf{U}_i^- + [\mathbf{M}_4 + \bar{\boldsymbol{\rho}}_- + \tfrac{1}{2}\tau^-(\mathbf{I} - \boldsymbol{\gamma}^{--})]\mathbf{U}_{i-1}^- =$$
$$= \tau(1 - \varpi)\mathbf{B}^- + \tfrac{1}{2}\tau^- \boldsymbol{\gamma}^{-+}\mathbf{U}_{i-1}^+ + \tfrac{1}{2}\tau^+ \boldsymbol{\gamma}^{-+}\mathbf{U}_i^+ , \tag{45}$$

where $\mathbf{I}$ is the identity matrix.

Let $\mathbf{U}_{i-1}^+$ and $\mathbf{U}_i^-$ are the intensities of the incident radiation and $\mathbf{U}_i^+$ and $\mathbf{U}_{i-1}^-$ are the intensities of the output radiation, then Equations (44) and (45) can be written as

$$\begin{bmatrix} \mathbf{U}_i^+ \\ \mathbf{U}_{i-1}^- \end{bmatrix} = \mathbf{K}^{-1} \begin{bmatrix} \mathbf{M}_3 + \bar{\boldsymbol{\rho}}_- - \tfrac{1}{2}\tau^-(\mathbf{I} - \boldsymbol{\gamma}^{++}) & \tfrac{1}{2}\tau^+ \boldsymbol{\gamma}^{+-} \\ \tfrac{1}{2}\tau^- \boldsymbol{\gamma}^{-+} & \mathbf{M}_2 - \bar{\boldsymbol{\rho}}_+ - \tfrac{1}{2}\tau^+(\mathbf{I} - \boldsymbol{\gamma}^{--}) \end{bmatrix} \begin{bmatrix} \mathbf{U}_{i-1}^+ \\ \mathbf{U}_i^- \end{bmatrix} +$$
$$+ \mathbf{K}^{-1}\tau(1 - \varpi) \begin{bmatrix} \mathbf{B}^+ \\ \mathbf{B}^- \end{bmatrix} . \tag{46}$$

Equation (46) may be compared with the principle of interaction (see Peraiah, 1984) given by

$$\begin{bmatrix} \mathbf{U}_i^+ \\ \mathbf{U}_{i-1}^- \end{bmatrix} = \begin{bmatrix} \mathbf{t}(i, i-1) & \mathbf{r}(i-1, i) \\ \mathbf{r}(i, i-1) & \mathbf{t}(i-1, i) \end{bmatrix} \begin{bmatrix} \mathbf{U}_{i-1}^+ \\ \mathbf{U}_i^- \end{bmatrix} + \begin{bmatrix} \Sigma_{i-1/2}^+ \\ \Sigma_{i-1/2}^+ \end{bmatrix} , \tag{47}$$

and obtain the reflection and transmission operators $r(i, i-1)$, $r(i-1, i)$, $t(i, i-1)$, and $t(i-1, i)$ together with the internal source terms $\Sigma_{i-1/2}^+$ and $\Sigma_{i-1/2}^-$.

We list them below for $\varpi = 0$ (non-scattering case):

$$\mathbf{r}(i, i-1) = \mathbf{r}(i-1, i) = 0 , \tag{48}$$
$$\mathbf{t}(i, i-1) = \boldsymbol{\Delta}^+ \mathbf{A} , \tag{49}$$
$$\mathbf{t}(i-1, i) = \boldsymbol{\Delta}^- \mathbf{D} , \tag{50}$$
$$\boldsymbol{\Sigma}_{i-1/2}^+ = \tau^+ \boldsymbol{\Delta}^+ \mathbf{B}^+ , \tag{51}$$
$$\boldsymbol{\Sigma}_{i-1/2}^- = \tau^- \boldsymbol{\Delta}^- \mathbf{B}^- , \tag{52}$$
$$\boldsymbol{\Delta}^+ = [\mathbf{M}_1 - \bar{\rho}_+ + \tfrac{1}{2}\tau^+ \mathbf{I}]^{-1} , \tag{53}$$

$$\Delta^- = [\mathbf{M}_4 + \bar{\rho}_- + \tfrac{1}{2}\tau^- \mathbf{I}]^{-1}, \tag{54}$$

$$\mathbf{A} = [\mathbf{M}_3 + \bar{\rho}_- - \tfrac{1}{2}\tau^- \mathbf{I}], \tag{55}$$

$$\mathbf{D} = [\mathbf{M}_2 - \bar{\rho}_+ - \tfrac{1}{2}\tau^+ \mathbf{I}]. \tag{56}$$

The internal field for the non-scattering media is given by

$$\mathbf{U}_i^+ = \mathbf{V}_{i-1/2}^+, \tag{57}$$

$$\mathbf{U}_{i-1}^- = \mathbf{t}(i-1, i)\mathbf{U}_i^- + \mathbf{V}_{i-1/2}^-, \tag{58}$$

$$\mathbf{V}_{i-1/2}^+ = \mathbf{t}(i, i-1)\mathbf{V}_{i-3/2}^+ + \mathbf{\Sigma}_{i-1/2}^+, \tag{59}$$

$$\mathbf{V}_{i-1/2}^- = \mathbf{\Sigma}_{i-1/2}^-; \tag{60}$$

with the initial conditions

$$\mathbf{U}_1^+(\mu_j) = 0 \quad \text{and} \quad \mathbf{U}_i^-(\mu_j) = 0. \tag{61}$$

If we compare the solution of the internal field given in Equations (57) to (60) with those given in Peraiah (1984), we note the simplicity of the scheme presented here. In the next section we shall present results and their discussion.

3. Results and Discussion of the Results

The solution of the transfer equation described in Equations (57) to (60) are presented in Figures 2 to 9 at different depths in the atmosphere. The initial conditions are

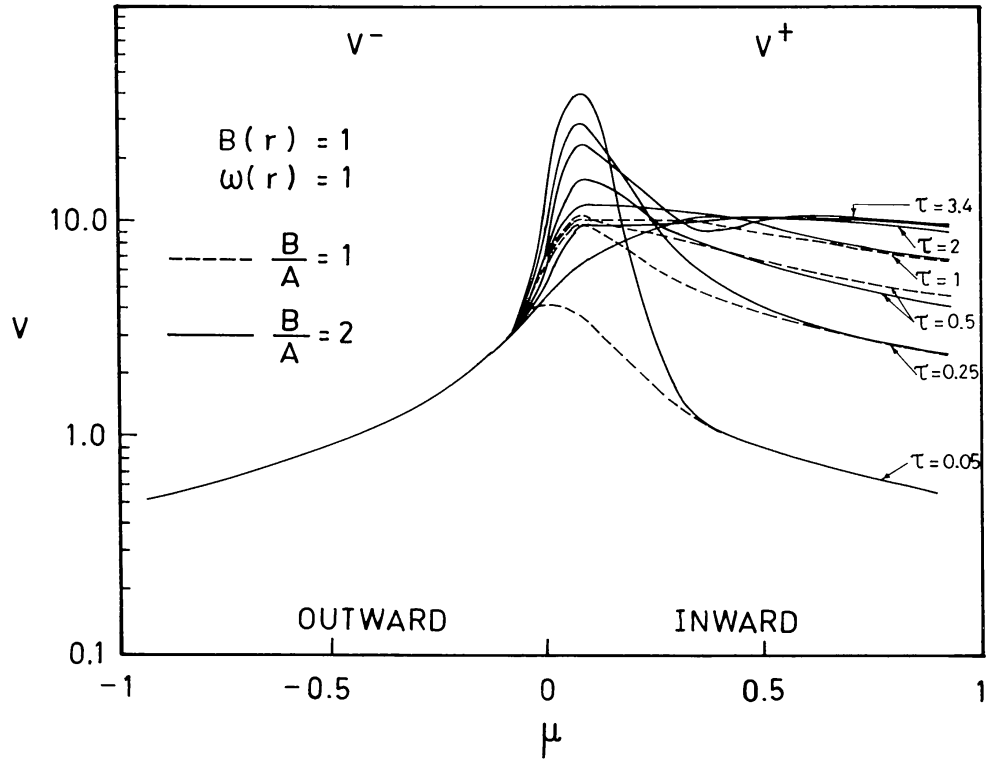

Fig. 2. Angular distribution of the source vectors v^+ and v^- for $B(r) = 1$ and $B/A = 1$ and 2.

described in Equation (61). These initial conditions imply that no radiation is incident from either side of the atmosphere. We have mainly calculated how the radiation of the internal emission is transferred. In the figures we have described the angular distribution of the source vectors v^- and v^+ and the specific intensities u^- and u^+ for various values of the Planck function and the parameter B/A, where B and A are the outer and inner radii of the medium. $B/A = 1$ implies plane parallel geometry and $B/A > 1$ represents spherically symmetric geometry.

In Figure 2, the source vectors v^- and v^+ are described for a constant Planck function $B(r) = 1$ and $B/A = 1$ and 2. In all the figure we have set ϖ, the albedo for single scattering equal to 0. We have assumed that the optical depth is constant at all radial points in this case. It is interesting to see that the emission of radiation which is directed outwards is constant throughout the atmospheres, although the emission of radiation directed towards the centre of the sphere varies with depth. More radiation is directed towards the centre of the star and the deeper layers emit more radiation which is directed inwards. However, there is a peak around $\mu = 0$ and the vectors v^- and v^+ are symmetric around this peak. The curvature factor which arises in the case of $B/A = 2$ does not seem to change the radiation field in the deeper layers. But, however, at $\tau = 0.05$ there are large differences between plane parallel and spherically symmetric cases around $\mu = 0$. The difference between the two cases at $\mu = 0$ is reduced gradually as we go deep into the atmosphere and the curves become graphically unresolvable. In Figure 3 we have described the specific intensities u^- and u^+ directed outwards and

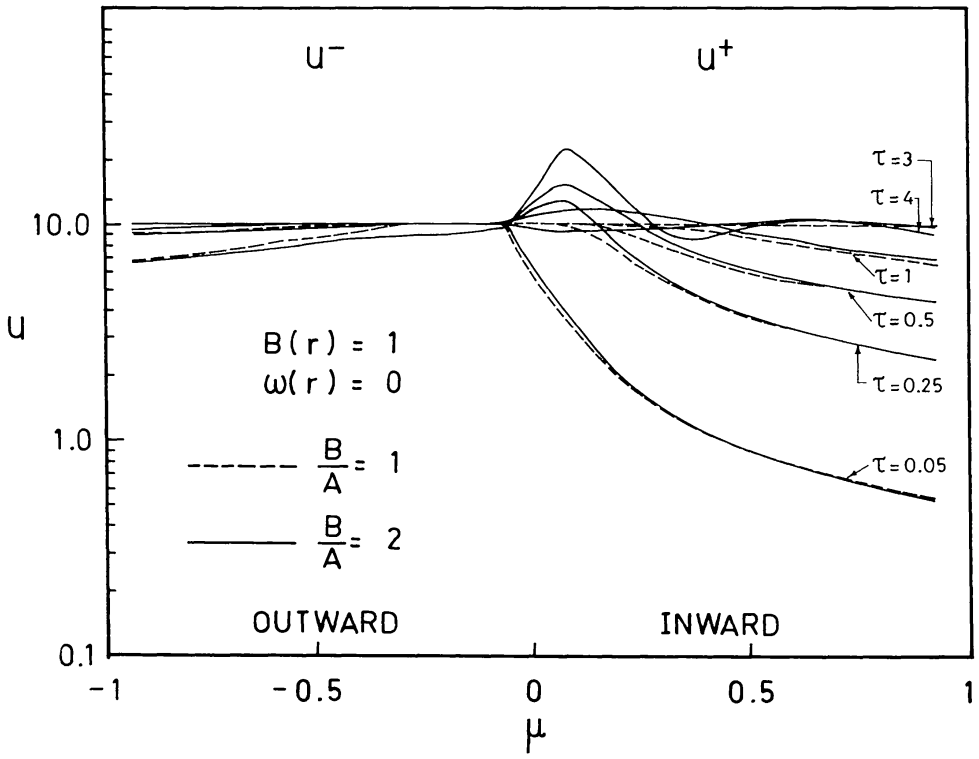

Fig. 3. Angular distribution of the intensities u^+ and u^- for $B(r) = 1$ and $B/A = 1$ and 2.

inwards, respectively. These intensities correspond to the source vectors given in Figure 2. We have given the results for both plane parallel and spherical symmetric cases. We see that the differences are not as conspicuous as shown by those in Figure 2. However, there are some similarities among the results given in these two figures.

In Figure 4, the source vectors v^- and v^+ are described for a medium with constant optical depth and with the Planck function varying as $1/r^2$. Again, here, we see a peaking pattern around $\mu = 0$. The radiation directed outwards depends on the depth where the radiation is emitted. It is emitted unlike the source vectors described in Figure 2 for a constant Planck function. More radiation is emitted at deeper layers than that emitted in the outer layers. From the outer layers little radiation is directed outwards. This is physically understandable because of the fact that the Planck function is a smaller in the outer layers and larger in the inner layers. There is another interesting feature in this that the plane parallel case will not give any variation in the radiation directed outwards while spherical symmetric case gives depth dependent radiation field. We also notice that plane parallel geometry gives more radiation than spherically symmetric geometry. However, there is tremendous amount of variation in the radiation directed inwards both in the plane parallel and spherical symmetric geometries. Again, here, the plane parallel geometry gives the higher estimation of radiation field compared to that of the spherically-symmetric geometry. The radiation that is emitted in the deeper layers is larger than that emitted in the outer layers. In the outermost layers more radiation is directed outwards compared to that directed inwards. In Figure 5 we plotted the specific

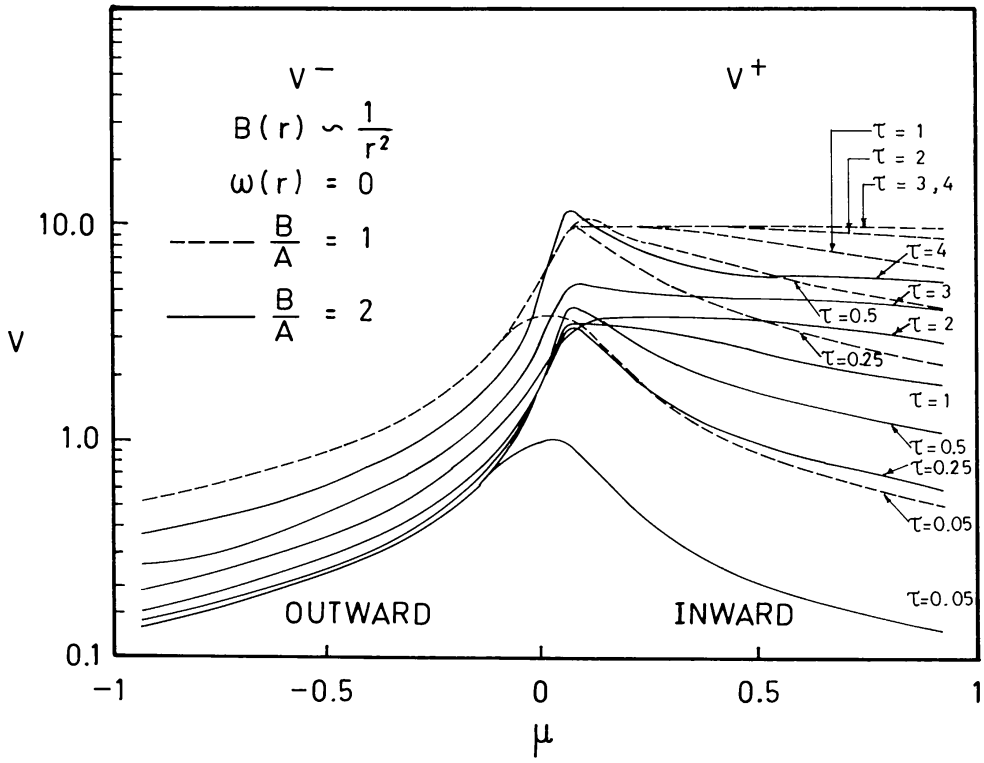

Fig. 4. Angular distribution of the source vectors v^+ and v^- for $B(r) \sim 1/r^2$ and $B/A = 1$ and 2.

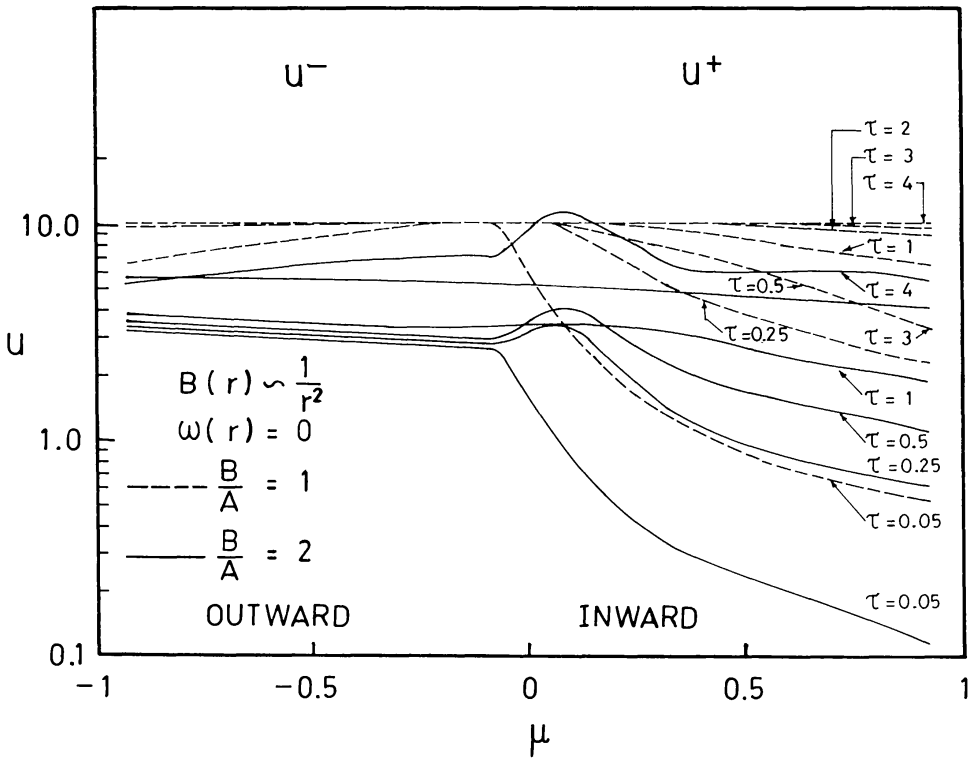

Fig. 5. Angular distribution of intensities u^+ and u^- for $B(r) \sim 1/r^2$ and $B/A = 1$ and 2.

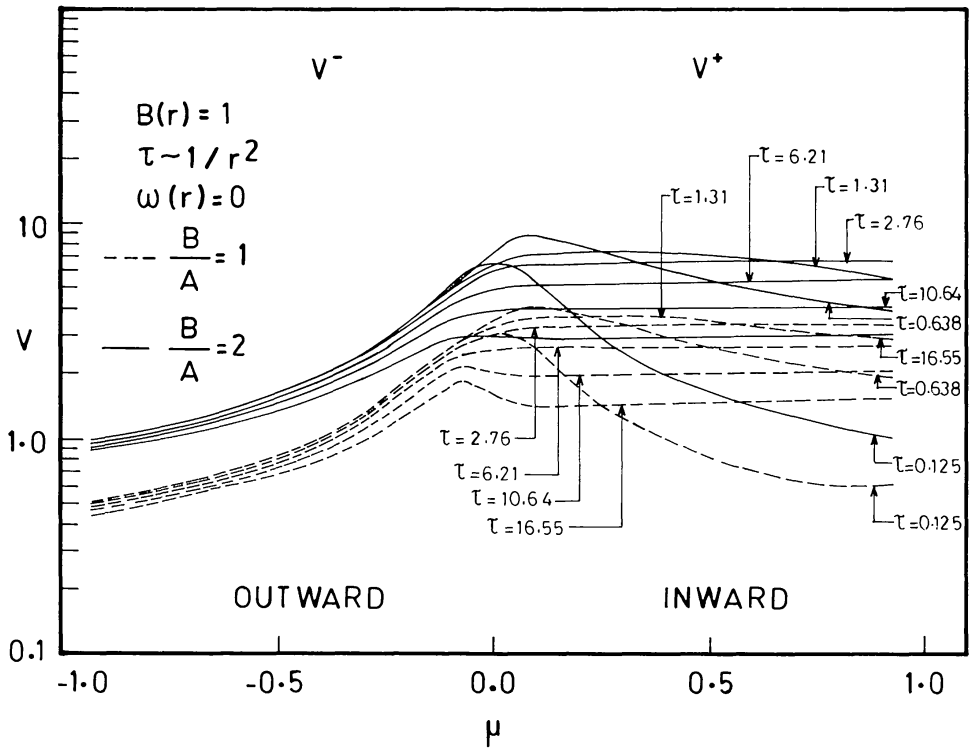

Fig. 6. Angular distribution of the source vectors for $B(r) = 1$ and $B/A = 1$ and 2. The optical depth τ varies as $1/r^2$.

intensities in the two directions, for the two cases of $B/A = 1$ and 2 with Planck function changing as $1/r^2$. These results seem to be a reflection of the variation in the source vectors v^- and v^+ shown in Figure 4. Here we have again assumed that the optical depth is constant though out the medium. The interesting phenomenon is that there is a peaking of the radiation aorund $\mu = 0$ at few internal points in the spherical atmospheres. The plane parallel atmospheres does not show this peaking phenomenon. There is more radiation going outwards than that going inwards. This phenomenon is true throughout the medium.

In Figure 6 we have presented results for both plane parallel and spherical symmetric geometries with the optical depth changing as $1/r^2$ and with a constant Planck function. The results shown in this figure are almost a reversal of the results shown in Figure 4 in which we have plotted source vector for a constant optical depth throughout the atmospheres. The source vectors shown in this figure (Figure 6) show a variation similar to that shown by the vectors given in Figure 4. But source vectors corresponding to the plane parallel case also show a depth dependance in the radiation directed outwards which is similar to those in the spherical case. The source vectors in the plane parallel case are all smaller than those in the spherically symmetric case in both the directions. In Figure 7 we have plotted the specific intensities corresponding to the source vectors given in Figure 6. Here we see the same type of variation as we see in the previous figure, although the intensities remain constant at some of the internal layers both in plane

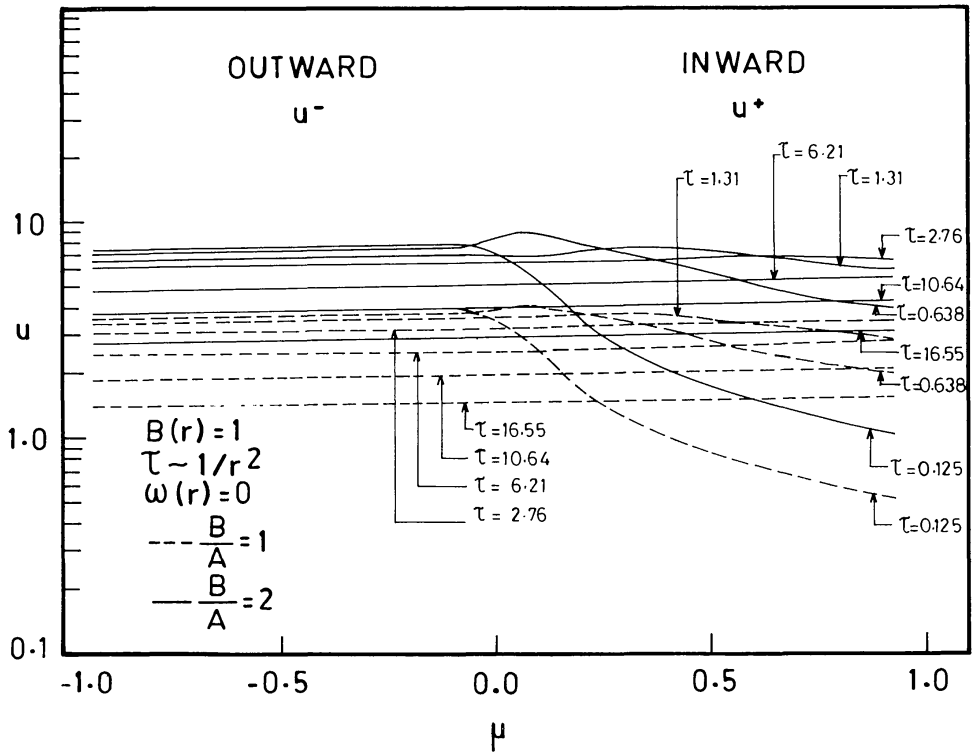

Fig. 7. Angular distribution of intensities u^+ and u^- for $B(r) = 1$ and $B/A = 1$ and 2. The optical depth varies as $1/t^2$.

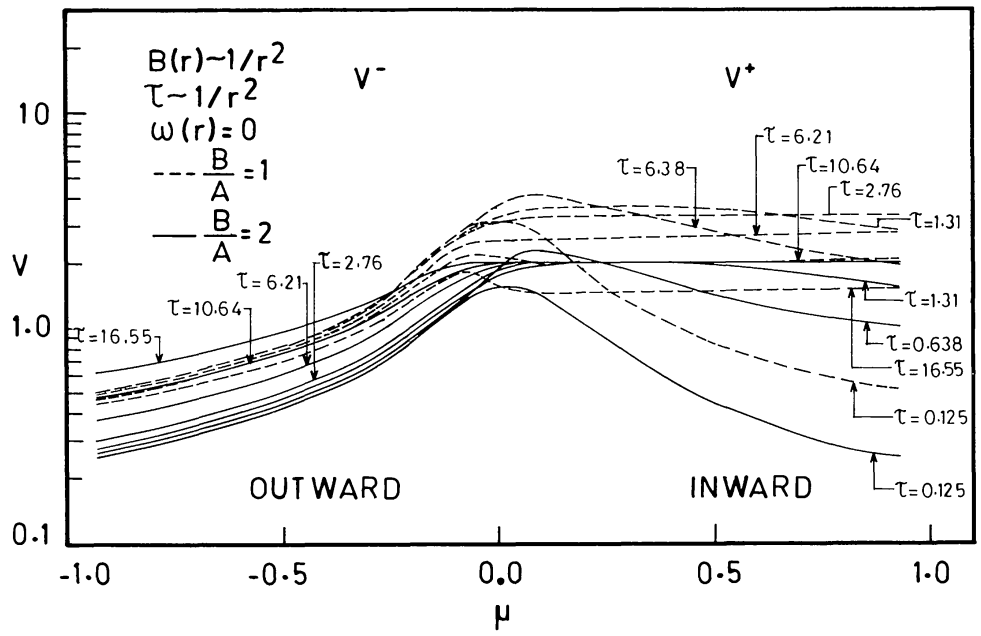

Fig. 8. Angular distribution of the source vectors for $B(r) \sim 1/r^2$, $\tau(r) \sim 1/r^2$, and $B/A = 1$ and 2.

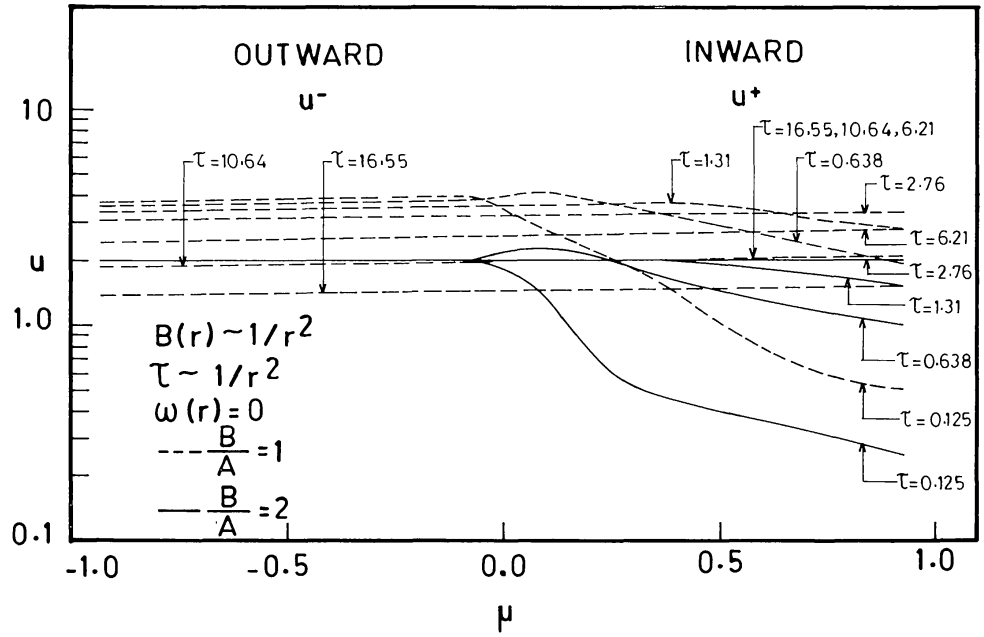

Fig. 9. Angular distribution of the intensities u^+ and u^- for $B(r) \sim 1/r^2$, $\tau(r) \sim 1/r^2$, and $B/A = 1$ and 2.

parallel and spherical symmetric geometries. Again, more radiation is emitted in the spherical case than in the plane parallel case.

In Figure 8 we have plotted source vectors of a medium in which the optical depth and Planck function are changing as $1/r^2$. The changes are quite similar to the results given in the previous figures although more radiation is emitted in the plane parallel

geometry than in the spherically symmetric case. In Figure 9 we have plotted the specific intensities corresponding to the source vectors given in Figure 8. These results appear to be quite similar to those given in Figure 7, although the plane parallel geometry appears to emit more radiation than the spherically symmetric approximation.

References

Lathrop, K. D. and Carlson, B. G.: 1967, *J. Comp. Physics* **2**, 173.
Lathrop, K. D. and Carlson, B. G.: 1971, *J. Quant. Spectrosc. Radiat. Transfer* **11**, 921.
Peraiah, A.: 1984, in W. Kalkofen (ed.), 'Discrete Space Theory of Radiative Transfer', *Methods in Radiative Transfer,* Cambridge University Press, New York.